SPECIAL 3D-TLM CORNER NODES FOR SINGULAR FIELD REGIONS

Giampaolo Tardioli°, Lucia Cascio, Mario Righi, and Wolfgang J.R. Hoefer°

°NSERC/MPR Teltech Research Chair in RF Engineering
Department of Electrical and Computer Engineering, University of Victoria,
Victoria, B.C. V8W 3P6, CANADA, email: tardioli@ece.uvic.ca

Abstract

A novel procedure to incorporate the static field configuration at field singularities into a 3D-TLM mesh is proposed. The procedure is systematic and consists in a modification of the scattering algorithm of the corner node. The modified cell imposes the correct singular field in the vicinity of a conducting edge using the information of the surrounding field evolution. The results for canonical resonators are consistent with those obtained with standard TLM simulation with cell size five to six times smaller.

Introduction

Space discrete methods such as Finite Difference Frequency Domain (FDFD), Finite Difference Time Domain (FDTD), Transmission Line Matrix (TLM) and Finite Element Methods (FEM), are currently used for solving a wide variety of fields problems [1]. The computational domain is discretized in a finite number of elementary cells where the electromagnetic field is assumed to have a simple behavior, very often linear. This assumption fails to accurately model sharp features, where highly nonuniform fields are present. This is typically the case of corners and edges, where the electromagnetic fields are singular. We refer to the resulting error as “coarseness error”.

In time domain methods, a comparison between the dispersion and the coarseness error reveals that the coarseness error is the dominant source of inaccuracies in most of the practical cases and represents the most severe limitation to the maximum admissible cell size [2],[3].

A direct solution to reduce the coarseness error is to use an extremely fine mesh, but this quickly leads to unacceptable memory and time requirements. A better approach is to use a variable or multigrid mesh, so that a higher resolution can be obtained in that region. In this case the resources would be still larger than those of a uniform coarser mesh fixed by the dispersion error only.

Solutions based on a local modification of the standard time domain algorithm have been proposed in order to embed the edge properties in one or more coarse cells surrounding the corner [4-9].

In this paper we present a novel approach to incorporate knowledge of the static field behavior in the vicinity of singularities in a three-dimensional TLM mesh. The procedure is systematic and does not require optimization of the correcting elements. As a result, relatively coarse TLM meshes may be used to obtain highly accurate results, within the dispersion error, across a wide frequency range.

Theoretical Background

Close to edges the spatial derivatives of the fields are much larger than the time derivatives, so that the latter may be neglected in Maxwell’s equations. Therefore the propagation effects are negligible and the electromagnetic field is essentially static. The singular behavior of the electromagnetic field at an edge follows from the requirement that the total energy near the edge must remain finite [10],[11]. Consider the perfectly conducting edge depicted in Fig. 1. The finite energy condition imposes that the **E** and **H** field components normal to the corner become singular, while the **E** and **H** tangential components remain finite.

In particular, for a knife wedge (α=0), the y-field components can be expressed as: [12]

$$E_y = \alpha(t)\, r^{1/2} \sin\left(\frac{\phi}{2}\right) + \beta(t) \cdot r \cdot \sin(\phi) + \gamma(t)\, r^{3/2} \sin\left(\frac{3\phi}{2}\right) + \ldots \quad (1)$$

0-7803-4603-6/97/$5.00 (c) IEEE

$$H_y = c_0(t) + c_1(t) \cdot r^{1/2} \cdot \sin\left(\frac{\phi}{2}\right) + c_2(t)\, r \sin(\phi) + \ldots \quad (2)$$

Considering Maxwell's equations written in the cylindrical coordinate system *y*-r-ϕ, we obtain:

$$\frac{\partial H_r}{\partial y} - \frac{\partial H_y}{\partial r} = \varepsilon_0 \frac{\partial E_\phi}{\partial t} \qquad \frac{\partial E_r}{\partial y} - \frac{\partial E_y}{\partial r} = -\mu_0 \frac{\partial H_\phi}{\partial t} \quad (3)$$

where Hy and Ey in the vicinity of the corner are given by (1), and (2).

Edge Singularity, TM-Polarization

Consider the case of the knife edge embedded in a TLM mesh as depicted in Fig. 2.

We want to implement the equations (3) including the edge condition (1) and (2) at the three TLM link lines. In particular for the TM^y polarization (H_y=0), we have:

$$\mu_0 \frac{\partial H_\phi\left(\frac{\Delta}{2}, \phi, t\right)}{\partial t} = \frac{\partial E_y\left(\frac{\Delta}{2}, \phi, t\right)}{\partial r} - \frac{\partial E_r\left(\frac{\Delta}{2}, \phi, t\right)}{\partial y} \quad (4)$$

Replacing the time derivative with the central difference scheme, and recalling the mapping between voltages and fields between link lines in the 3D-SCN node [13], we can determine the following relationship for the voltage pulses incident at the points 1,2,3:

$$(V_k^r - V_k^i) - (V_{k-1}^r - V_{k-1}^i) = Z_0 \frac{\Delta l \Delta t}{\mu_0} \cdot \left(\frac{\partial E_y}{\partial r} - \frac{\partial E_r}{\partial y}\right) \quad (5)$$

where Z_0 is link line characteristic impedance, V_k^r are the voltage pulses incident on the points 1,2,3 from *the corner node* and V_k^i are the voltage pulses incident on the points 1,2,3 from *the external nodes* at the k^{th} iteration. Note that the correction algorithm exploits the reflected and incident voltages at the corner node during the previous time step, thus increasing the information contained in that cell.

The second term of equation (5) can be evaluated using the static expansion (1). Considering the first three terms of the expansion, the derivative of E_y becomes:

$$\frac{\partial E_y\left(\frac{\Delta l}{2}, \phi, t\right)}{\partial r} = \frac{1}{2}\alpha(t)\left(\frac{\Delta l}{2}\right)^{-\frac{1}{2}} \sin\left(\frac{\phi}{2}\right) + \beta(t)\sin(\phi) + \frac{3}{2}\gamma(t)\left(\frac{\Delta l}{2}\right)^{\frac{1}{2}} \sin\left(\frac{3}{2}\phi\right) + \ldots \quad (6)$$

where the coefficients α(t), β(t), γ(t) are unknown. Their value can be determined by evaluating the electric field E_y at the three adjacent nodes at each time step and solving a linear system. The solution gives values of α, β, γ, as a function of the voltages E^1_y, E^2_y, E^3_y (Fig. 3):

$$\alpha = \frac{(\sqrt{2}E_y^1 + 2E_y^2 + \sqrt{2}E_y^3)}{4r_0} \qquad \beta = \frac{(E_y^3 - E_y^1)}{2r_0^2}$$
$$\gamma = -\frac{(E_y^1 - \sqrt{2}E_y^2 + E_y^3)}{2\sqrt{2}r_0^3} \qquad r_0 = \sqrt{\Delta l} \quad (7)$$

The modified scattering procedure for higher-order approximation is obtained by solving (5) with respect to V_k^r and using (7):

$$G(\phi, k) = \frac{1}{2}\alpha(k\Delta t)\left(\frac{\Delta l}{2}\right)^{-\frac{1}{2}} \sin\left(\frac{\phi}{2}\right) + \beta(k\Delta t)\sin(\phi) + \left(\frac{3}{2}\gamma(k\Delta t)\left(\frac{\Delta l}{2}\right)^{\frac{1}{2}} \sin\left(\frac{3}{2}\phi\right)\right)$$
$$V_k^r = V_k^i + V_{k-1}^r - V_{k-1}^i + \frac{\Delta l^2}{2} \cdot \left(G(\phi, k) - \frac{\partial E_r}{\partial y}\right) \quad (8)$$

where $\partial E_r / \partial y$ can be evaluated with a central difference scheme.

Edge Singularity, TE-Polarization

The calculations for the TE^y (E_y=0) polarization are carried out in a similar manner as per the TM^y polarization. Considering the first of the equations (3), and the edge condition (2), together with the mapping between voltages and fields between link lines in the SCN node, we obtain:

$$(V_k^r + V_k^i) - (V_{k-1}^r + V_{k-1}^i) = -\frac{\Delta l \Delta t}{\varepsilon} \cdot \left(\frac{\partial H_y}{\partial r} - \frac{\partial H_r}{\partial y}\right) \quad (Port-3)$$
$$(V_k^r + V_k^i) - (V_{k-1}^r + V_{k-1}^i) = \frac{\Delta l \Delta t}{\varepsilon} \cdot \left(\frac{\partial H_y}{\partial r} - \frac{\partial H_r}{\partial y}\right) \quad (Port-1, 2) \quad (9)$$

where the derivative of H_y can be approximated as:

$$\frac{\partial H_y}{\partial r} = \frac{1}{2}c_1(t)\left(\frac{\Delta l}{2}\right)^{-\frac{1}{2}} \cos(\phi) + c_2(t)\cos\left(\frac{3}{2}\phi\right) + \ldots \quad (10)$$

and $\partial H_r/\partial y$ with a central difference scheme. The values of c_1 and c_2 as a function of the magnetic fields H_y^1, H_y^2, H_y^3 (Fig. 3) are:

$$c_1 = \frac{(H_y^3 - H_y^1)}{\sqrt{2\Delta l}} \qquad c_2 = -\frac{(H_y^1 - 2H_y^2 + H_y^3)}{2\Delta l} \qquad (11)$$

Results

In order to validate the proposed approach for the two different polarizations, we have implemented the algorithm in the 3D-SCN node, and computed the first resonant frequency of the cavities depicted in Fig. 4 and Fig. 5. The first structure is a rectangular cavity with an asymmetric inductive iris in the center. The second structure is a parallel plate waveguide resonator with an asymmetric capacitive iris in the middle. In both situations the new method has been compared with results available in the literature [14] and with those obtained with the standard TLM algorithm with increasingly small discretization steps (Table 1 and Table 2). A very coarse mesh has intentionally been considered in order to highlight the coarseness error and its correction. Even with a very coarse mesh the introduction of the static-field correction yields an improvement in the accuracy with negligible impact on the computational time; the percentage error is reduced from 3.8% to 1% in the case of the TM polarization, and from 10% to 0.3% in the case of TE polarization. These results are consistent with those obtained with a standard TLM algorithm with cell sizes five to six times smaller with a significant saving in computational effort.

In the analysis of discontinuities where TE and TM polarizations are uncoupled, instabilities were never encountered. When the two polarizations are excited simultaneously, the proposed method still increases the accuracy, but long term instabilities have been observed and their nature is currently under investigation.

Conclusion

A novel systematic procedure to incorporate static field configuration into a 3D-TLM mesh has been proposed. The method introduces the correct field singularity by exploiting the previous incident and reflected link-line voltages surrounding the corner node. The procedure requires negligible additional operations and leads to a saving in computational time and memory of two orders of magnitude. Future work is directed towards the application of the method to the analysis of planar circuits.

Acknowledgments

This research has been funded by the Natural Sciences and Engineering Research Council of Canada, the Science Council of British Columbia, MPR Teltech Inc. of Burnaby, B.C., and the University of Victoria.

References

[1] T. Itoh ed., “Numerical Techniques for Microwave and Millimeter-Wave Passive Structures”, New-York, John Wiley & Sons, 1989.

[2] L. de Menezes, W. J. R. Hoefer, “Accuracy of TLM Solutions of Maxwell’s Equations”, *IEEE MTTS Symposium Digest*, 1996, pp.1019-1022.

[3] P. Mezzanotte, L. Roselli, C. Huber, H. Zscheile, W. Heinrich, “On the Accuracy of the Finite -Difference Method Using Mesh Grading”, *IEEE MTTS Symposium Digest*, 1995, pp. 781-784.

[4] G. Mur, “The Modeling of Singularities in the Finite-Difference Approximation of the Time-Domain Electromagnetic-Field Equations”, *IEEE Trans. Microwave Theory and Tech.*, vol. 29, no. 10, pp 1073-1077, Oct. 1981.

[5] D. B. Shorthouse, C. J. Railton, “The Incorporation of Static Field Solutions Into the Finite Difference Time Domain Algorithm”, *IEEE Trans. Microwave Theory and Tech.*, vol. 40, Oct, no. 5, pp 986-994, May 1992.

[6] U. Mueller, P. So, W. J. R. Hoefer, “The Compensation of coarseness error in 2D TLM modeling of microwave structures”, *IEEE MTTS Symposium Digest*, 1992, pp. 373-376.

[7] L. Herring, W. J. R. Hoefer, “Compensation of Coarseness Error in TLM Modeling of Microwave Structures with the Symmetrical Condensed Node”, *IEEE MTTS Symposium Digest*, 1995, Paper TU1B-2, pp. 23-26.

[8] L. Cascio, G. Tardioli, T. Rozzi, W. J. R. Hoefer, “A Quasi-Static Modification of TLM at Knife Edge and 90° Wedge Singularities”, *IEEE MTTS Symposium Digest*, 1996, pp. 443-446.

[9] B. Bader, P. Russer, “Modelling of Edges and Corners in the Alternating Transmission Line matrix (ATLM) Scheme”, *Electronics Letters*, vol. 32, no. 20, pp 1897-1898, Sept. 1996.

[10] J. Meixner, “The Behavior of Electromagnetic Fields at Edges”, *IEEE Transactions on Antennas*

and Propagations, vol. 20, no. 4, pp 442-446, July 1972.

[11] J. Van Bladel, *Singular Electromagnetic Fields and Sources*, IEEE Press, 1995.

[12] D. S. Jones, *The Theory of Electromagnetics*, Oxford, England, Pergamon, 1964.

[13] P. B. Johns, "A Symmetrical Condensed Node for the TLM Method", *IEEE Trans. Microwave Theory and Tech.*, vol. 35, pp 370-377, Apr. 1987.

[14] N. Marcuvitz, *Waveguide Handbook*, Boston Technical Publishers, 1964.

Figures

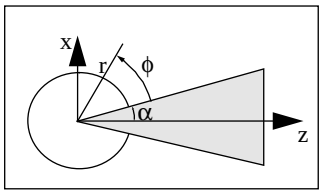

Fig. 1 Perfectly conducting wedge

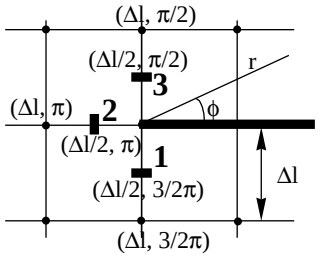

Fig. 2 Knife edge in a TLM mesh; the edge is placed on TLM nodes

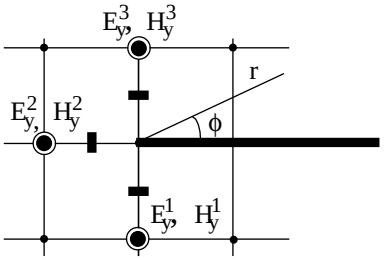

Fig. 3 Configuration for the evaluation of the expansion coefficients

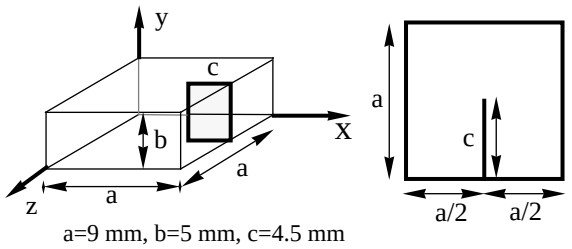

a=9 mm, b=5 mm, c=4.5 mm

Fig. 4 Resonant cavity in rectangular waveguide with inductive coupling

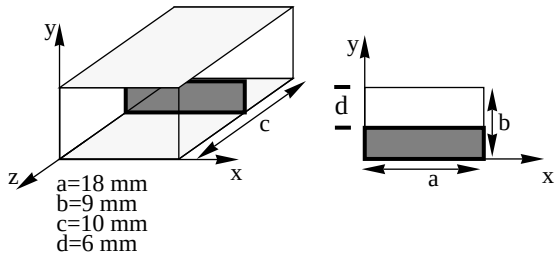

Fig. 5 Resonant cavity in parallel plate waveguide with capacitive coupling

Table 1: Inductive Iris (Frequency in GHz)

Δl	1 mm	1/3 mm	1/5 mm
TLM	31.732	31.062	30.922
Marcuvitz	30.560	-	-
Static Correction	30.889	-	-

Table 2: Capacitive Iris (Frequency in GHz)

Δl	1 mm	1/3 mm	1/5 mm	1/11 mm
TLM	11.175	11.935	12.105	12.260
Marcuvitz	12.475	-	-	-
Static Correction	12.510		-	-